Available at www.sciencedirect.com

ScienceDirect

journal homepage: www.elsevier.com/locate/modo

Myosin heavy chain isoform expression in adult and juvenile mini-muscle mice bred for high-voluntary wheel running

Robert J. Talmadge [a,*], Wendy Acosta [b], Theodore Garland Jr. [b]

[a] Department of Biological Sciences, California State Polytechnic University, Pomona, CA 91768, USA
[b] Department of Biology, University of California, Riverside, CA 92521, USA

ARTICLE INFO

Article history:
Received 20 March 2014
Received in revised form
21 August 2014
Accepted 23 August 2014
Available online 16 September 2014

Keywords:
Artificial selection
Fiber-type
Mouse
Myosin
Running
Skeletal muscle

ABSTRACT

The myosin heavy chain (MyHC) isoform composition of locomotor and non-locomotor muscles of mini-muscle mice were assessed at the protein and mRNA levels in both adult and juvenile (21 day old) mice. Mini-muscle mice are one outcome of a replicated artificial selection experiment in which four lines of mice were bred for high voluntary wheel running (HR lines). Two of the lines responded with an increase in frequency of a single nucleotide polymorphism in an intron in the MyHC-2b gene (*myh4*) that when homozygous causes a dramatic reduction in triceps surae mass. We found that both locomotor and non-locomotor muscles of adult mini-muscle mice displayed robust reductions, but not elimination, of the MyHC-2b isoform at both the protein and mRNA levels, with commensurate increases in MyHC-2x and sometimes MyHC-2a, as compared with either a line of HR mice that does not display the mini-muscle phenotype or inbred C57Bl6 mice. Immunohistochemical analyses revealed that locomotor muscles of mini-muscle mice contain fibers that express the MyHC-2b isoform, which migrates normally in SDS-PAGE gels. However, these MyHC-2b positive fibers are generally smaller than the surrounding fibers and smaller than the MyHC-2b positive fibers of non-mini-muscle mice, resulting in characteristically fast muscles that lack a substantial MyHC-2b positive (superficial) region. In contrast, the masseter, a non-locomotor muscle of mini-muscle mice contained MyHC-2b positive fibers that stained more lightly for MyHC-2b, but appeared normal in size and distribution. In adults, many of the MyHC-2b positive fibers in the mini-muscle mice also display central nuclei. Only a small proportion of small MyHC-2b fibers in mini-muscle mice stained positive for the neural cell adhesion molecule, suggesting that anatomical innervation was not compromised. In addition, weanling (21 day old), but not 5 day old mice, displayed alterations in MyHC isoform content at both the protein and mRNA levels, including reductions in MyHC-2b and elevations in the neonatal (a.k.a. perinatal) isoform of MyHC. Collectively, these data demonstrate that the alterations in the expression of MyHC-2b are not restricted to locomotor muscles and therefore are not caused simply by any possible alterations in locomotor activity (e.g., reduced general activity in home cages). The differences in MyHC composition do not appear to result from a defect in innervation of the MyHC-2b fibers, but may result from an inefficient neonatal-to-2b MyHC isoform transition during development and are consistent with a selective lack of maturation of MyHC-2b fibers caused by reduced expression of the MyHC-2b (*myh4*) gene.

* Corresponding author. Department of Biological Sciences, California State Polytechnic University, Pomona, CA 91768, USA. Tel.: +1 909 869 3025; fax: +1 909 869 4078.
E-mail address: rjtalmadge@csupomona.edu (R.J. Talmadge).

http://dx.doi.org/10.1016/j.mod.2014.08.004
0925-4773/

1. Introduction

Alterations in the amount of daily contractile activity can have a profound influence on skeletal muscle. Reductions in neuromuscular activation, such as occur following spinal cord injury, space flight, and hindlimb suspension generally result in fiber transitions towards faster phenotypes (Talmadge, 2000). In contrast, conditions associated with elevations in contractile activity, such as chronic electrical stimulation, exercise, and functional overload are associated with fiber transformation towards slower phenotypes (Pette and Vrbova, 1992; Roy et al., 1991; Schiaffino and Reggiani, 2011).

Although significant strides in understanding the cellular and molecular mechanisms associated with the activity-based regulation of muscle fiber type transformation have occurred over the past two decades, the mechanisms associated with the genetic (and heritable) regulation of adult fiber phenotype have been largely unexplored. A unique animal model for understanding some of the factors that contribute to the genetic regulation of muscle fiber type is the high-activity "mini-muscle" mouse (Garland et al., 2002; Swallow et al., 1998). The high-activity mice (designated as HR for high running) are the product of a replicated artificial selection experiment in which mice were (and continue to be) bred for high voluntary wheel-running activity. The selection protocol entailed the generation of 4 lines of mice that were bred for high wheel running during a 6-day period of wheel access administered at ~6–8 weeks of age. At an apparent selection limit, the HR mouse lines run daily distances that are ~2.5× greater than those of four non-selected control lines (Careau et al., 2013; Garland et al., 2011). Two of the HR lines display a morphological phenotype designated as mini-muscle because the triceps surae muscle mass is approximately 50% of control levels (Garland et al., 2002; Houle-Leroy et al., 2003). This phenotype is inherited as an autosomal recessive (Garland et al., 2002; Hannon et al., 2008; Hartmann et al., 2008) and is caused by a single nucleotide polymorphism (SNP) in the 709-bp intron located between exons 11 and 12 of the 2b-MyHC (*myh4*) gene on chromosome 11 (Kelly et al., 2013). The SNP consists of a C-to-T transition at position 67,244,850 (Kelly et al., 2013). In one of the HR mini-muscle lines (lab-designated as line 3), the mini-muscle morphological phenotype has gone to fixation, i.e., all mice express the phenotype (Syme et al., 2005). The second HR mini-muscle line (designated as line 6) remains polymorphic and follows typical Mendelian inheritance of the mini-muscle phenotype.

One interesting feature of the "mini-muscle" mice is that they show a pronounced reduction in the fast glycolytic (i.e., type 2B) fiber type in locomotor muscles that normally contain this fiber type (Bilodeau et al., 2009; Guderley et al., 2006; McGillivray et al., 2009b). Accompanying the reduction in the 2B fiber type is a corresponding reduction in expression of the myosin heavy chain (MyHC)-2b isoform (Bilodeau et al., 2009; Guderley et al., 2006; McGillivray et al., 2009b).

It is clear that the MyHC isoform expressed in a single muscle fiber is a primary factor associated with determining the speed-related contractile properties of that fiber (Canepari et al., 2010), and is highly correlated with other metabolic properties of the fiber (Rivero et al., 1998, 1999). Four adult MyHC isoforms are generally expressed in adult rodent muscle fibers: (from slowest to fastest) types MyHC-I (gene designation *myh7*), MyHC-2a (*myh2*), MyHC-2x (*myh1*), and MyHC-2b (*myh4*). Muscles with high maximal contractile speeds, including fast muscles like the gastrocnemius and tibialis anterior, generally have a high complement of MyHC-2b fibers which are typically located at the superficial portion of the muscle, whereas muscles with low maximal contractile speeds, including the soleus and adductor longus, generally have a high compliment of MyHC-I and MyHC-2a fibers. In association with the reduction in the 2B phenotype, significant alterations in muscle contractile performance (McGillivray et al., 2009b; Syme et al., 2005) and in whole-animal performance (reduced maximal sprint-running speed and an increased cost of transport (Dlugosz et al., 2009)) are observed in the mini-muscle individuals.

At present, it is not known if the alterations in fiber type in the mini-muscle mice are restricted to locomotor muscles or if they occur more widely (among most or all muscles of the body). Because HR mice, including mini-muscle individuals, have increased locomotor activity in home cages when housed without wheels (Malisch et al., 2009), it is theoretically possible that the alteration in locomotor muscle fiber type could result from elevated locomotor muscle contractile activity during their ontogenetic development. If so, then the cause of the mini-muscle phenotype would be viewed as an indirect pleiotropic effect, rather than a direct genetic effect. The reduced triceps surae mass of mini-muscle individuals becomes apparent only at approximately two weeks of age, which is before much locomotion occurs (Middleton et al., 2008), but mice do move before this age, e.g., when trying to gain access to nursing. Therefore, to determine if the fiber type differences in the mini-muscle mice are restricted to locomotor muscles or are more generalized, this study assessed MyHC isoform expression at the protein and mRNA levels in several locomotor and non-locomotor muscles in adult mini-muscle mice and two control groups, an HR line that does not express the mini-muscle phenotype (line 8) and inbred C57Bl6 mice from an outside source. This study also assessed if the changes in MyHC isoform expression were restricted to adult mice or observable at earlier ages, specifically 5 day (neonates) and 21 day old (juvenile) mice.

2. Materials and methods

2.1. *Animals and experimental procedure*

The groups included: (1) Line 3 HR mini-muscle mice; (2) Line 7 and 8 HR (non-mini-muscle) mice; and (3) C57Bl6NHsd mice obtained directly from Harlan Laboratories (Indianapolis, IN, USA). For analyses in adult mice, six mice from each group were utilized. For analyses of neonatal (p5) and juvenile (p21), three to six mini-muscle (line 3) mice and three to six non-mini-muscle mice (lines 7 and 8) were utilized. Muscles and muscle groups representing locomotor muscles (including the triceps surae, quadriceps, soleus, and trapezius) and non-locomotor muscles (including the tongue, masseter, and diaphragm) were dissected, cleaned of connective tissue, and frozen in isopentane chilled by liquid nitrogen. The triceps surae and quadriceps were chosen as representative muscles in-

Table 1 – Primary antibodies used for immunohistochemistry.

Antibody designation	Specificity	Antibody class	Source
Slow (NOQ7.5.4d)	MyHC-I	IgG	Sigma-Aldrich, Inc. St. Louis, Mo, USA
S58	MyHC-I	IgA	Developmental Studies Hybridoma Bank Iowa City, IA, USA
SC-71	MyHC-2a	IgG	Developmental Studies Hybridoma Bank Iowa City, IA, USA
F30	MyHC-2b	IgG	Developmental Studies Hybridoma Bank Iowa City, IA, USA
BF-F3	MyHC-2b	IgM	Developmental Studies Hybridoma Bank Iowa City, IA, USA
Dev (NCL-MHCd)	MyHC-embryonic	IgG	Vector Laboratories Burlingame, CA, USA
Dys-2	Dystrophin (sarcolemma)	IgG	Vector Laboratories Burlingame, CA, USA
AB5032	Neural cell adhesion molecule (NCAM)	IgG	Millipore Inc. Billerica, MA, USA

volved in hindlimb appendage locomotion. The trapezius was chosen as an upper torso axial muscle involved in stabilizing the scapula during locomotor tasks. The tongue and masseter were chosen as muscles involved in tasks completely unrelated to locomotion, i.e., mastication, and the diaphragm was chosen as a muscle involved in respiration, although its activity is related to the degree of locomotor activity. All animal procedures were approved by the University of California, Riverside and the California State Polytechnic University Institutional Animal Care and Use Committees.

2.2. *Electrophoresis of myosin heavy chain isoforms*

Myofibrillar protein was extracted from one-half of the frozen muscles (Thomason et al., 1986). Protein content of the myofibrillar extracts was quantified using the Bradford technique. The extracts were then diluted to a final concentration of 8 ng/μl in SDS-PAGE sample buffer (Laemmli, 1970). A total of 160 ng of myofibrillar protein (20 μl) were loaded per lane onto high resolution sodium-dodecyl sulfate polyacrylamide gels for the separation of MyHC isoforms. For the separation of mouse MyHC isoforms a modification of the method of Talmadge and Roy was used (Talmadge and Roy, 1993). The modifications followed those previously described by Mizunoya et al (Mizunoya et al., 2008), with the exception that the gels (both stacking and separating portions) contained 30% glycerol and not 35% as recommended (Mizunoya et al., 2008). Following electrophoresis, the gels were silver stained (Silver Stain Plus™, Biorad, Hercules, CA, USA), imaged with a FluorChem™ gel imaging system (Alpha Innotech, CA, USA), and band densities were quantified using the line scan mode. Band densities were converted to MyHC isoform proportions.

2.3. *Myosin heavy chain isoform immunohistochemistry*

A portion of some of the frozen muscles was used for the immunohistochemical localization of specific MyHC isoforms in single muscle fibers following the procedures used previously by (Talmadge et al., 1995) using the MyHC isoform-specific monoclonal antibodies detailed in Table 1. Additional antibodies included antibodies for labeling the fiber sarcolemma, Dys-2 for dystrophin and for the localization of the neural cell adhesion molecule (NCAM) for identification of denervated muscle fibers (see Table 1). For fluorescence immunocytochemistry Alexa-488 and Alexa-546 conjugated secondary antibodies (Invitrogen, Grand Island, NY, USA) were used and sections were mounted with mounting media containing DAPI for the visualization of nuclei. Muscle cross-sections were viewed using a fluorescence microscope, Retiga 2000RV camera (QImaging, Surrey, BC Canada), and QCapture Pro software (QImaging, Surrey, BC, Canada).

For some immunohistochemical evaluations of MyHC isoform composition, a tricolor immunofluorescence technique based on the procedure of Ribaric and Cebasek (2013) was used. This technique involved the simultaneous detection of 3 MyHC isoform in a single tissue section using specific antibodies for MyHC-I, MyHC-2a, and MyHC-2b. By default, unstained fibers would contain MyHC-2x. However, the possibility of co-expression of MyHC-2x and another MyHC isoform in the same fiber would go undetected with this method. Briefly 10 μm cryostat sections were incubated in succession with (1) PBS (to rehydrate) for 10 min, (2) blocking solution (20% goat serum in PBS) for 30 min, (3) 1° antibody cocktail (see Table 2), (4) PBS rinse for 10 min, (5) 2° antibody cocktail (see Table 2), (6) PBS rinse for 10 min, (7) mount coverslips. Using appropriate filter cubes, images were then obtained at each of the three fluorescence channels and composite images generated using Olympus Microsuite® showing MyHC-2b fibers as green, MyHC-2a fibers as blue, and MyHC-I fibers as red.

2.4. *Analysis of myosin heavy chain isoform mRNAs*

Skeletal muscle mRNA was prepared and DNase-treated using RNeasy micro kits (Qiagen Sciences, Valencia, CA, USA) and diluted to 100 ng/μl with nuclease-free H_2O. The RNA (1 μg) was reverse transcribed to cDNA with Invitrogen (Carlsbad, CA, USA) SuperScript III reverse transcriptase in a final volume of 40 μl. For the gel-based assay of MyHC mRNA isoforms, 1 μl of the cDNA was used for each PCR reaction. The PCR primers and reactions followed the previously published protocol of Sartorius

Table 2 – Antibody cocktails for tricolor immunofluorescence.

MyHC isoform	1° mAb Cocktail	2° mAb Cocktail	Pseudocolor
I	600 µl Antibody S58 (IgA, 1:5)	30 µl anti-mIgA – TRITC conjugate (SERA Labs)	red
2a	6 µl Antibody SC71 (IgG, 1:500)	30 µl anti-mIgG-Alexa 647 (Invitrogen)	blue
2b	50 µl Antibody F3 (IgM, 1:30)	6 µl anti-mIgM-Alexa 488 (Invitrogen)	green
–	2344 µl Blocking solution	2934 µl PBS	–
–	3000 µl Final volume	3000 µl Final Volume	–

Note: MyHC-2x fibers would be unstained and appear black. Also, if MyHC-2x was co-expressed in a single fiber along with another MyHC isoform, its presence would be undetected with this technique. However, this technique allows for a fast reliable method for detecting the adult MyHC-isoforms in rodent muscle.

et al. (1998). The PCR product bands were quantified after electrophoresis in 2% agarose gels in the presence of ethidium bromide. Band intensities were quantified using a FluorChem™ gel imaging system (Alpha Innotech, CA, USA). Real-time RT-PCR analyses for MyHC isoforms were performed using a DNA Engine Opticon 2 real-time PCR fluorescence detection system (Biorad, Hercules, CA). One microliter of cDNA was used per 20 µl reaction. Each reaction also contained 10 µl of Applied Biosystems (Invitrogen, Carlsbad, CA) TaqMan® gene expression 2× master mix and 1 µl of the appropriate 20× primer probe combination (see Table 3). Cycling conditions were as follows: 50 °C for 2 min, 95 °C for 10 min, then 40 cycles of 95 °C for 20 seconds, 60 °C for 1 min, and a fluorescence detection step. After the reactions were complete, cycle thresholds were established, and relative expression levels (relative to either housekeeping gene, β-2-microglobulin or β-actin as specified) determined using the delta delta CT method (Livak and Schmittgen, 2001).

2.5. *Statistical analysis*

All values are presented as means ± the standard error of the mean. Statistical comparisons among the three groups were performed using an analysis of variance (ANOVA) followed by the Student–Newman–Keuls method for pair-wise comparisons with significance designated as $p \leq 0.05$. Where appropriate (2-group comparisons), Student's t-tests were performed with significance set at $p \leq 0.05$. Because the myosin heavy chain isoform data are presented as proportional data, the relative proportions of one isoform are dependent on the proportions of the other three isoforms. Therefore, we limited our pairwise comparisons to only the fast MyHC isoforms for gel electrophoretic data.

Table 3 – TaqMan® Gene Expression Probe/Primers.

Gene	Primer/probe designation
myh1 (MyHC-2x/d)	Mm01332489.m1
myh2 (MyHC-2a)	Mm01332564.m1
myh3 (MyHC-embryonic)	Mm01332463.m1
myh4 (MyHC-2b)	Mm01332518.m1
myh7 (MyHC-I)	Mm01319006.g1
myh8 (MyHC-neonatal)	Mm01329494.m1
β-2-microglobulin	Mm00437762.m1
β-actin	Mm00607939.s1

TaqMan® Gene Expression Probe/Primer combinations were obtained from Invitrogen.

3. Results

As shown in Fig. 1, an electrophoretic assessment of MyHC isoform content revealed that both locomotor and non-locomotor muscles which normally contain a substantial proportion of MyHC-2b (i.e., quadriceps, trapezius, masseter, tongue, and diaphragm) showed a clear and statistically significant reduction in the proportion of MyHC-2b in mini-muscle mice (line 3) when compared to C57Bl6 and HR line 8 mice. The only muscle not to show a reduced MyHC-2b proportion in mini-muscle mice was the soleus, which contains a very small proportion (generally less than 5%) of MyHC-2b in control C57Bl6 and HR line 8 mice, and which actually shows a slightly greater mass in mini-muscle mice versus wildtype individuals (Burniston et al., 2013; Guderley et al., 2006; McGillivray et al., 2009a; Syme et al., 2005). In general, the loss in MyHC-2b was compensated by an elevation in MyHC-2x and in one case MyHC-2a as well (quadriceps). In addition, the master muscle contained neonatal MyHC (see the MyHC band just below MyHC-2x) which was also present in trace amounts in the diaphragm. Also, the HR line 8 mice showed similar MyHC isoform distributions as the C57Bl6 mice, confirming their use as controls for MyHC isoform expression. In total, SDS-PAGE analyses revealed no statistical differences in MyHC isoform protein content between HR line 8 and C57Bl6 mice for any muscle examined.

MyHC isoform mRNA analyses using a gel-based reverse transcriptase-polymerase chain reaction (RT-PCR) technique (using β-actin as a reference gene) of adult mini-muscle mice were performed on two muscles, the quadriceps (representing a locomotor muscle) and the tongue (a non-locomotor muscle). In both muscles the relative content of MyHC-2b mRNA was significantly reduced (Fig. 2). Curiously, MyHC-2x was decreased in HR Line-8 mice relative to C57Bl controls; however, the other adult MyHC isoform mRNAs were largely unchanged (Fig. 2). Real-time quantitative RT-PCR analyses also demonstrated a reduction in MyHC-2b mRNA levels in mini-muscle mice (Fig. 2C and F).

The electrophoretic and mRNA data were supported by qualitative immunohistochemical evaluation of MyHC isoform content of single muscle fibers in the triceps surae, particularly the gastrocnemius muscle (Fig. 3). For instance, the majority of gastrocnemius muscle fibers (deep region) of HR line 8 mice stained positively for MyHC-2b, along with a few that stained positively for MyHC-2a and none for MyHC-I (Fig. 3I). A few fibers were unstained for MyHCs-I, -2a and -2b

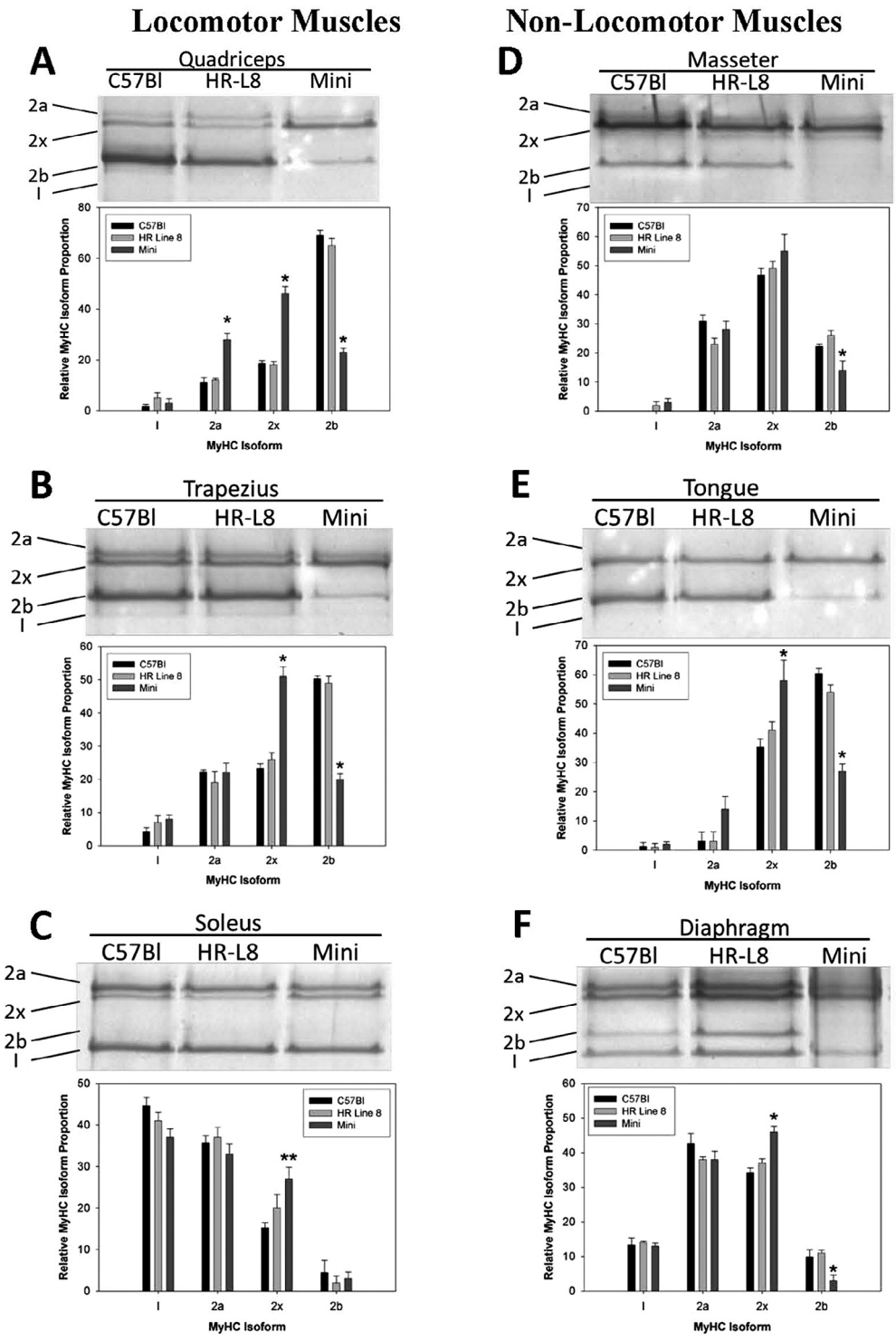

Fig. 1 – High resolution sodium dodecyl sulfate polyacrylamide (SDS-PAGE) gels and mean MyHC isoform proportions from locomotor muscles (A–C; quadriceps, trapezius, soleus) and non-locomotor muscles (D–F; masseter, tongue, diaphragm). Each gel contains a single representative sample from a C57Bl6 control (C57Bl), high-running line 8 (non-mini) (HR-L8) and high-running line 3 mini-muscle (Mini) mouse. The four adult MyHC isoform bands are identified to the left of each gel as follows: MyHC-2a (2a); MyHC-2x/d (2x); MyHC-2b (2b); and MyHC-I (I). In the associated bar graphs, muscles of C57Bl6 (dark bars), HR line 8 (non-mini) (light bars), and line 3 HR mini-muscle (Mini, intermediate bars) mice are shown. The bars represent the mean values +/– the SEM. The * denotes significantly different from C57Bl6 and HR line 8 mice at $p \leq 0.05$. The ** denotes significantly different from C57Bl6, but not HR line 8 mice at $p \leq 0.05$. Notice the relative reduction in MyHC-2b in the quadriceps, trapezius, masseter, tongue, and diaphragm muscles of the mini-muscle mice in comparison to the C57Bl6 and HR-L8 mice.

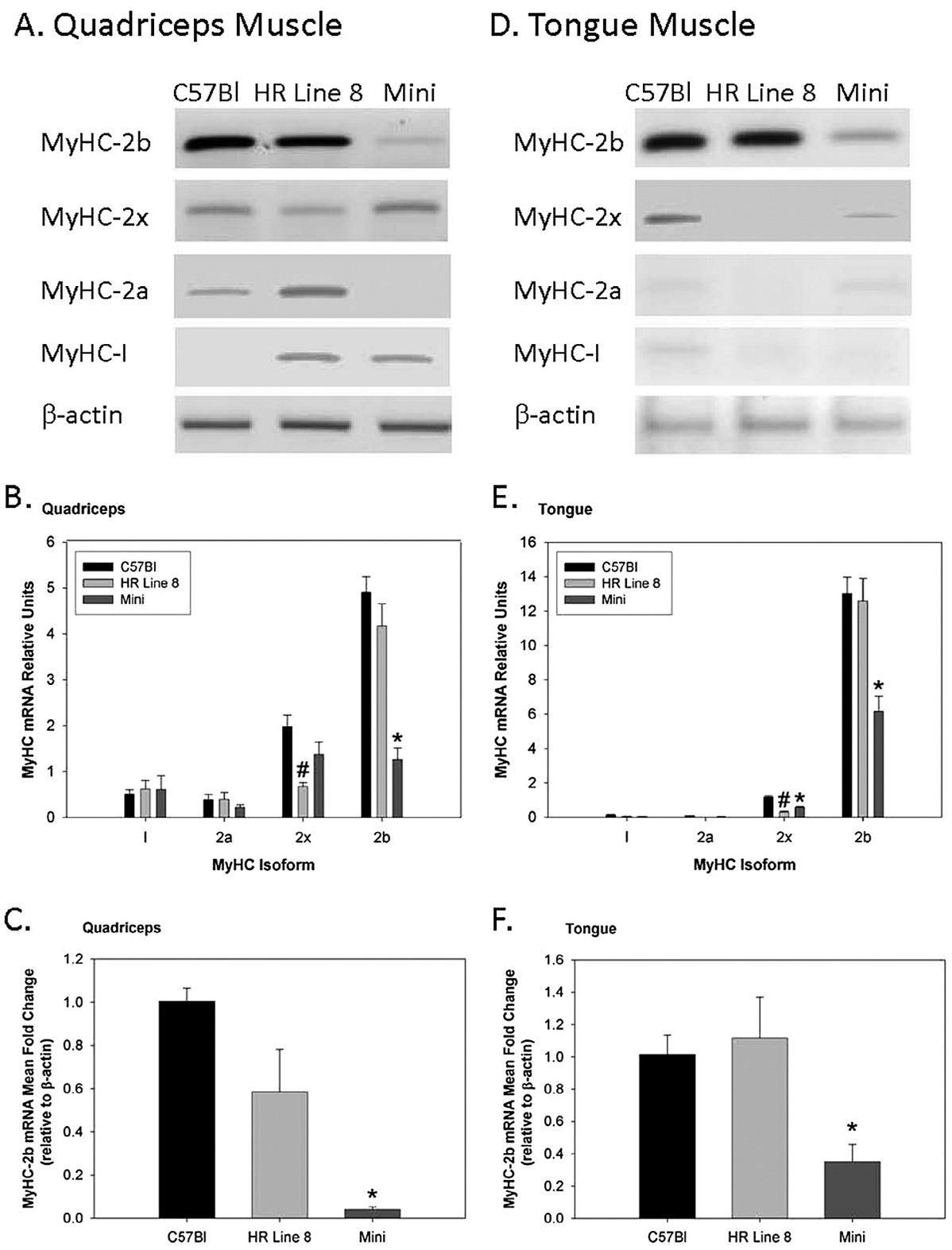

Fig. 2 – MyHC isoform mRNA levels in the quadriceps muscle group (locomotor muscle) and the tongue (non-locomotor muscle) of control (C57Bl and HR Line 8 mice) and mini-muscle mice (Mini). A gel-based reverse transcriptase polymerase chain reaction (RT-PCR) technique as described in Materials and Methods was performed and fragments separated on 2% agarose gels (A and D). Band intensities relative to β-actin are quantified in B and E. In addition, a real-time RT-PCR technique was also used to quantify MyHC-2b mRNA levels (C and F). The bars represent the mean values +/– the SEM. The asterisk denotes significantly different from both control groups and the #-sign denotes significantly different from C57Bl at $p \leq 0.05$.

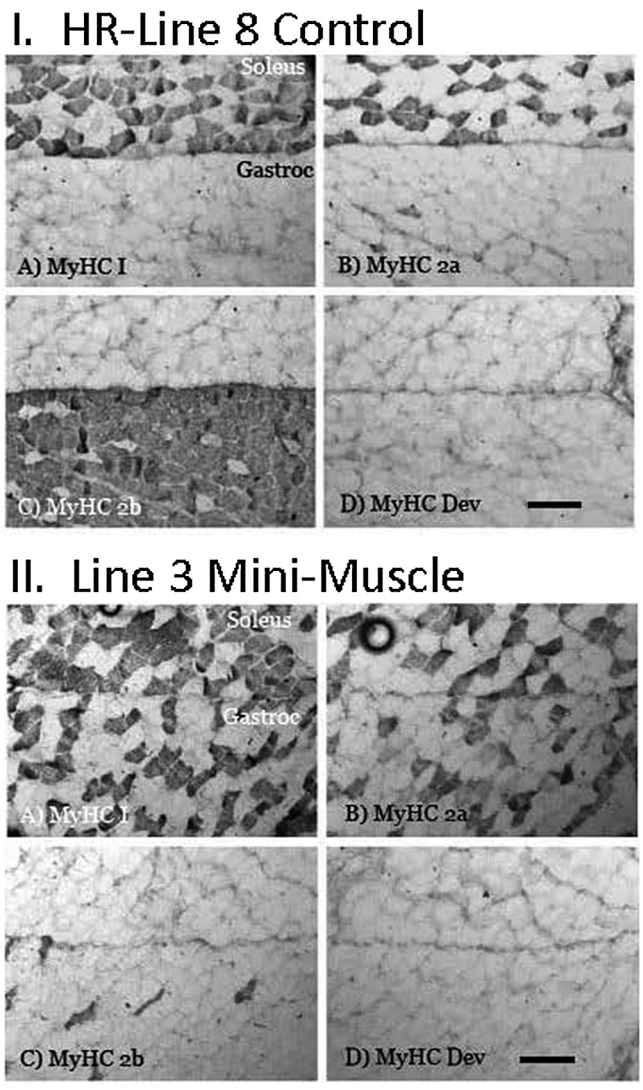

Fig. 3 – Representative serial triceps surae cross-sections stained immunohistochemically for the presence of MyHC isoforms from an HR line 8 (non-mini) mouse (I, top panel) and an HR line 3 mini-muscle mouse (II, bottom panel). (A) MyHC-I; (B) MyHC-2a (SC71); (C) MyHC-2b (F30); (D) Developmental (embryonic) MyHC. The regions of the gastrocnemius (gastroc) and the soleus, bottom and top, respectively, are shown in panel A. The scale bar in D represents 100 μm for all sections.

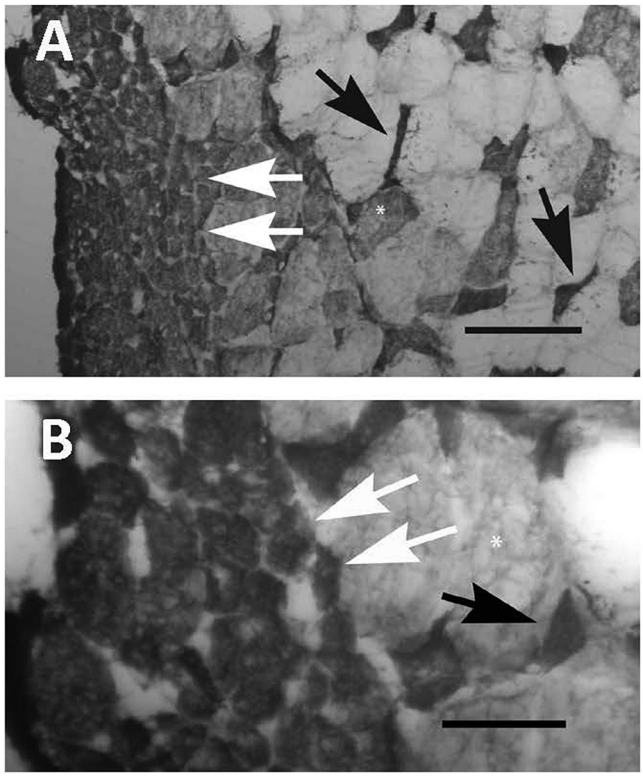

Fig. 4 – Representative triceps surae cross-sections (showing the superficial region of the medial gastrocnemius) from an HR line 3 mini-muscle mouse stained for MyHC-2b with antibody F30. (A) Low magnification (scale bar represents 100 μm). (B) High magnification (scale bar represents 50 μm). The black arrows in both A and B identify the relatively sparse MyHC-2b positive small 'angular' fibers present within the muscle belly. The twin parallel white arrows in both A and B identify the numerous MyHC-2b positive small 'rounded' fibers at the peripheral surface of the muscle.

and presumably contain MyHC-2x. In contrast, the deep region of the gastrocnemius of the mini-muscle mice (Fig. 3II) contained very few fibers that stained positive for MyHC-2b and many more that stained positive for MyHC-I and MyHC-2a, as well as many presumptive 2d/x fibers (unstained for MyHCs-I, -2a, and -2b). Thus, there is an apparent shift from MyHC-2b fibers towards those containing MyHC-2x and even MyHCs-2a and -I in the deep region of the gastrocnemius in mini-muscle mice.

A closer examination of the relatively few MyHC-2b positive fibers in the gastrocnemius of the mini-muscle mice revealed two categories of fibers with distinct morphological characteristics (Fig. 4). The first were observed within the deep/mid portions of the gastrocnemius, and these MyHC-2b positive fibers were generally small and 'angular' in appearance (fibers labeled with black arrows in Fig. 4). The second were typically located at the most superficial aspect of the muscle, and were small and 'rounded' in appearance (fibers labeled with twin parallel white arrows in Fig. 4). Curiously, the non-locomotor masseter muscle of mini-muscle mice displayed MyHC-2b positive fibers that stained lighter for MyHC-2b compared to non-mini muscle mice, but were similar in size to surrounding fibers, as well as to MyHC-2b fibers in non-mini muscle mice (Fig. 5).

Further evaluation of the small MyHC-2b positive fibers in the locomotor muscles of mini-muscle mice revealed that many of them (both 'angular' and 'rounded' fibers) contained central nuclei (Fig. 6, white arrows). As small, 'rounded', and centrally nucleated muscle fibers are frequently observed in denervated or degenerating and regenerating muscle (e.g., Whalen et al., 1990), as well as developing muscle (e.g., Condon et al., 1990), we assessed the levels of embryonic MyHC isoforms (an indicator of muscle regeneration and previous satellite cell activation) immunohistochemically in mini-muscle mice

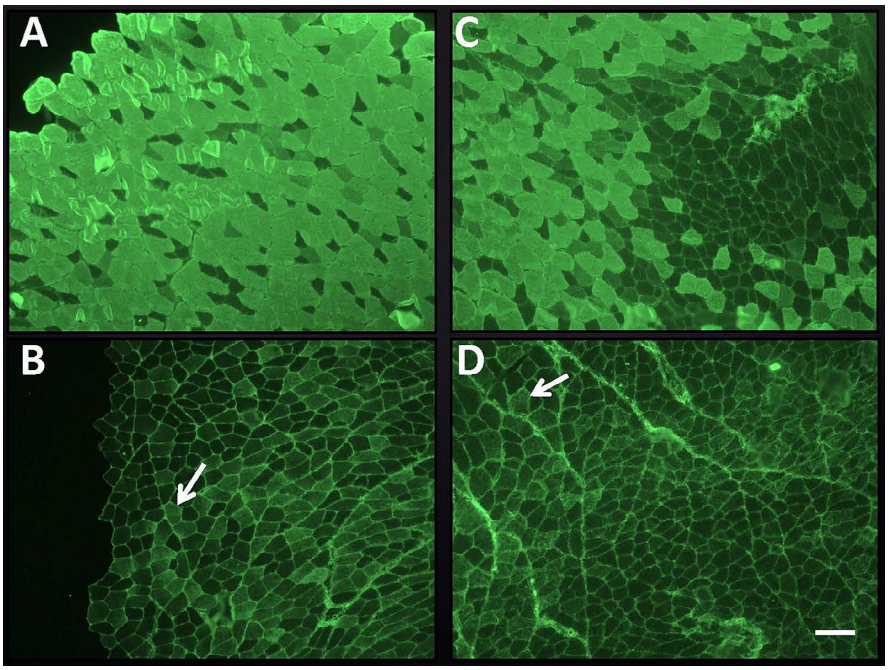

Fig. 5 – Representative cross-sections of the posterior end of the masseter muscle stained immunohistochemically for the presence of MyHC-2b. Panels (A) and (B) show the superficial region from an HR line 8 (non-mini) mouse and an HR line 3 mini-muscle mouse, respectively. Panels (C) and (D) show the deep region from an HR line 8 (non-mini) mouse and an HR line 3 mini-muscle mouse, respectively. The scale bar in D represents 100 μm for all sections.

(Fig. 3D), but found no fibers with embryonic MyHC. In addition, the potential for fiber denervation was evaluated by neural cell adhesion molecule (NCAM) staining, given that denervated muscle fibers display a distinct NCAM positive periphery (Gordon et al., 2009). The small 'angular' MyHC-2b positive fibers of the mini-muscle mice were uniformly devoid of NCAM staining (Fig. 7). In contrast, a small proportion of small rounded MyHC-2b and non-2b fibers showed distinct NCAM staining on the fiber periphery (Fig. 7C, see white arrows), indicative of some minor, but perhaps secondary, myofiber denervation.

To investigate the age at which differential expression of MyHC isoforms is observed in locomotor muscles of mini-muscle vs "control" (i.e., non-mini-muscle) mice the MyHC isoforms in both 5 (p5, neonatal mice, before the onset of MyHC-2b expression) and 21 (p21, juvenile mice, after the onset of MyHC-2b expression) day old mice. SDS-PAGE analyses revealed no differences in the expression of MyHC isoforms at p5 (Fig. 8A). In both mini-muscle (line 3) and non-mini-muscle (line 8) mice three bands were observed. One located slightly above MyHC-2a corresponds to MyHC-embryonic and one located slightly below MyHC-2x corresponds to MyHC-neonatal (for reference, see Agbulut et al., 2003). A third distinct protein band was observed, which did not correspond to other previously identified MyHC isoforms (see the band labeled N′ in Fig. 8A). The identity of this band is currently unresolved. Regardless, at p5, no differences in MyHC isoform content were observed between mini-muscle and non-mini-muscle mice and MyHC-2b was not detected at measureable levels.

In contrast, at p21, the expression of MyHC-2b at the protein level was clearly evident in non-mini-muscle mice, but significantly reduced (although still present) in mini-muscle mice (Fig. 8B). This reduction in MyHC-2b was evident for both the triceps surae and the quadriceps muscle groups (Fig. 8B–D). Real-time RT-PCR analyses of the six MyHC isoforms typically expressed at p21 at the mRNA level (using β-2-microglobulin as a reference house-keeping gene) showed a dramatic reduction in MyHC-2b mRNA (only 3% of non-mini) and a 3-fold elevation in MyHC-neonatal (Fig. 8E). Interestingly, there was also a ~50% reduction in MyHC-I mRNA in the p21 triceps surae of mini-muscle mice. Fluorescence immunohistochemistry for the adult MyHC isoforms revealed that both the triceps surae (not shown) and the quadriceps muscle groups of mini-muscle mice had smaller and fewer MyHC-2b fibers compared to non-mini muscle mice, as was shown previously for adults. For example, as shown in Fig. 9, the quadriceps of mini-muscle mice at p21 contained far fewer MyHC-2b positive (green) fibers. This resulted in a much smaller MyHC-2b positive superficial region in the rectus femoris and vastus lateralis muscles of the quadriceps (Fig. 9). The superficial vastus lateralis in non-mini-muscle mice contained virtually 100% MyHC-2b fibers, and this was decreased substantially in mini-muscle mice (Fig. 9C and D). The majority of fibers in the superficial region of mini-muscle mice appear to contain predominantly MyHC-2x (non-stained, black) based on tricolor immunofluorescence (Fig. 9C and D). The deeply located vastus intermedius also showed alterations in MyHC isoform content in mini-muscle mice, including reductions in MyHC-2b positive fibers (Fig. 10). In non-mini-muscle mice, the MyHC-2b positive fibers appeared to be larger than MyHC-2a (blue) or MyHC-I (red) positive fibers (Fig. 10A); whereas the few MyHC-2b positive fibers in

mini-muscle mice appeared to be smaller than MyHC-2a or MyHC-I positive fibers (Fig. 10B).

4. Discussion

The quantitative differences in MyHC isoform content in the mini-muscle mice are not specific to locomotor muscles (Guderley et al., 2006; present study), but appear as a more generalized alteration in fiber type and MyHC isoform expression among the entire skeletal musculature. This conclusion is based on the reduction in MyHC-2b shown in the non-locomotor masseter, tongue, and diaphragm muscles compared with wildtype C57Bl6 and HR line 8 mice. The trapezius muscle, which acts to stabilize the scapula and is likely involved in movements associated with the neck and head and therefore is not solely associated with locomotor function, also showed a clear reduction in MyHC-2b protein. Thus, non-locomotor muscles showed a clear reduction in MyHC-2b in the mini-muscle mice. The other HR line that was analyzed (line 8) had MyHC isoform distributions that were similar to C57Bl6 mice obtained from an outside source. Adult HR line 8 mice, like HR line 3 mini-muscle mice, have a high propensity for daily locomotor activity, both on wheels and in home cages when wheels are not present (Malisch et al., 2009). However, line 8 mice did not show the same reduction in MyHC-2b as mini-muscle mice. This result supports the idea that the alterations in MyHC isoform expression in mini-muscle mice are unrelated to increased daily activity during the developmental period, but instead are induced by molecular and cellular processes that are directly related to the SNP located in the MyHC-2b gene (Kelly et al., 2013).

The expression of a MyHC-2b protein of apparently normal molecular mass (see MyHC SDS-PAGE gels, Fig. 1) and that reacts with antibodies directed against normal MyHC-2b in some fibers within the mini-muscle mouse suggests that the reduction in MyHC-2b protein is likely not attributable to any alteration in the coding region of pre-mRNA or mature mRNA that encodes MyHC-2b (*myh4*). Thus the SNP at position 67,244,850 on chromosome 11 of the mouse (Kelly et al., 2013) does not appear to influence splicing of the MyHC-2b gene, but only the gene's maximal expression at the whole muscle level. Future studies will address the expression level in single muscle fibers.

Multiple potential cellular mechanisms could result in a reduced MyHC-2b expression in the mini-muscle mice. First, it is possible that the SNP could be present at an intronic cis-acting regulatory element that is necessary for high level MyHC-2b expression and that the C to T transition renders the element less functional (future studies will address this). In turn, this

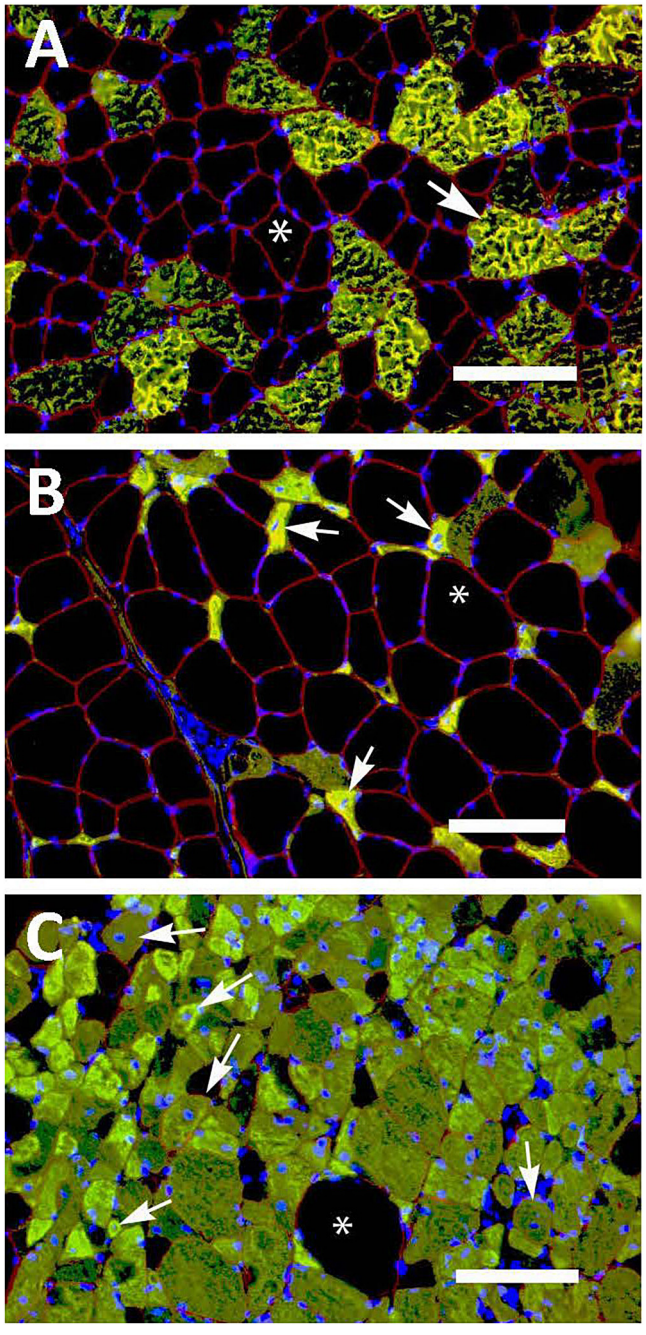

Fig. 6 – Representative triceps surae cross-sections showing: (A) the mid/deep-region of the gastrocnemius of an HR line 8 (non-mini) mouse; (B) the mid-region of the gastrocnemius of an HR line 3 mini-muscle mouse, and (C) the superficial region of the gastrocnemius of an HR line 3 mini-muscle mouse triple stained for MyHC-2b with antibody BF-F3 (yellow/green), dystrophin (demarks the fiber sarcolemma, red), and nuclei (blue). (A) As expected, in the non-mini-muscle mouse, the mid/deep-region of the gastrocnemius contains several large MyHC-2b positive fibers (white arrow) and several fibers that are negative for MyHC-2b (white asterisk). The myonuclei in the non-mini-muscle mouse are positioned at the fiber periphery (scale bar in A = 100 μm). (B) In the mini-muscle mouse, the mid-region of the gastrocnemius contains several small 'angular' MyHC-2b positive fibers, many with central nuclei (white arrows) and several fibers that are negative for MyHC-2b with peripheral nuclei (white asterisk) (scale bar in B = 50 μm). (C) In the superficial region of the gastrocnemius of the mini-muscle mouse, many small 'rounded' MyHC-2b positive fibers, many of which have central nuclei, are present (white arrows). This region contains a few fibers that are negative for MyHC-2b with peripheral nuclei (white asterisk) (scale bar in C = 50 μm).

would cause a reduction in transcription of the *myh4* gene resulting in a reduction in MyHC-2b mRNA, as we observed. The corresponding deficiency of MyHC-2b mRNA could potentially slow the synthesis of MyHC-2b protein and result in a reduced size of 2B fibers in locomotor muscles, due to insufficient MyHC protein synthesis in the 2B fibers. Interestingly, the mini-muscle mice share some characteristics with mice harboring a deletion of the *myh4* gene (MyHC-2b knockout mice, $2b^{-/-}$-mice). For instance, both mini-muscle and $2b^{-/-}$-mice have smaller body and muscle masses than wildtype individuals (Acakpo-Satchivi et al., 1997). Also, line 6 mini-muscle mice have an increased proportion of large fibers in the plantaris (Guderley et al., 2006), which is similar to the larger fibers observed in the $2b^{-/-}$-mice (Acakpo-Satchivi et al., 1997; Allen et al., 2001), particularly at the superficial region of the gastrocnemius (Allen et al., 2000). We speculate that in both animal models there is a selective hypertrophy of some of the remaining fibers that provides some degree of functional compensation for the loss ($2b^{-/-}$-mice) or reduced size (line 3 mini-muscle mice) of 2B fibers.

Second, the observation that MyHC-neonatal is up-regulated in mini-muscle mice at p21 (relative to non-mini-muscle mice) suggests that the typical ontogenetic transition from neonatal myosin to adult MyHC-2b in fast muscles (Adams et al., 1999; Adams et al., 2000; di Maso et al., 1999) may be disrupted in mini-muscle mice. A series of recent papers have highlighted the importance of natural anti-sense RNAs (NARs) in the regulation of the individual MyHC genes located in the fast MyHC gene cluster (which is located on chromosome 11 in mice, 10 in rats, and 17 in humans) (Haddad et al., 2007; Pandorf et al., 2006, 2012; Rinaldi et al., 2008). This gene cluster consists of six consecutive MyHC genes located in a "head to tail" orientation. In order, this cluster consists of *myh3* (embryonic), *myh2* (MyHC-2a), *myh1* (MyHC-2x/d), *myh4* (MyHC-2b), *myh8* (MyHC-neonatal), and *myh13* (MyHC-extraocular) (Yoon et al., 1992). Collectively, these papers have demonstrated the presence of bidirectional promoters located in between the coding regions of several of the genes in the cluster. The activation of any particular bidirectional promoter in the cluster would increase the expression of the protein-encoding mRNA for the downstream MyHC isoform and the non-encoding and inhibitory NAR for the upstream MyHC isoform, thus resulting in down-regulation of the upstream gene. As MyHC-2b precedes MyHC-neonatal with an intervening region of approximately 16.7 Kb in mice, it is possible that the SNP may somehow induce an

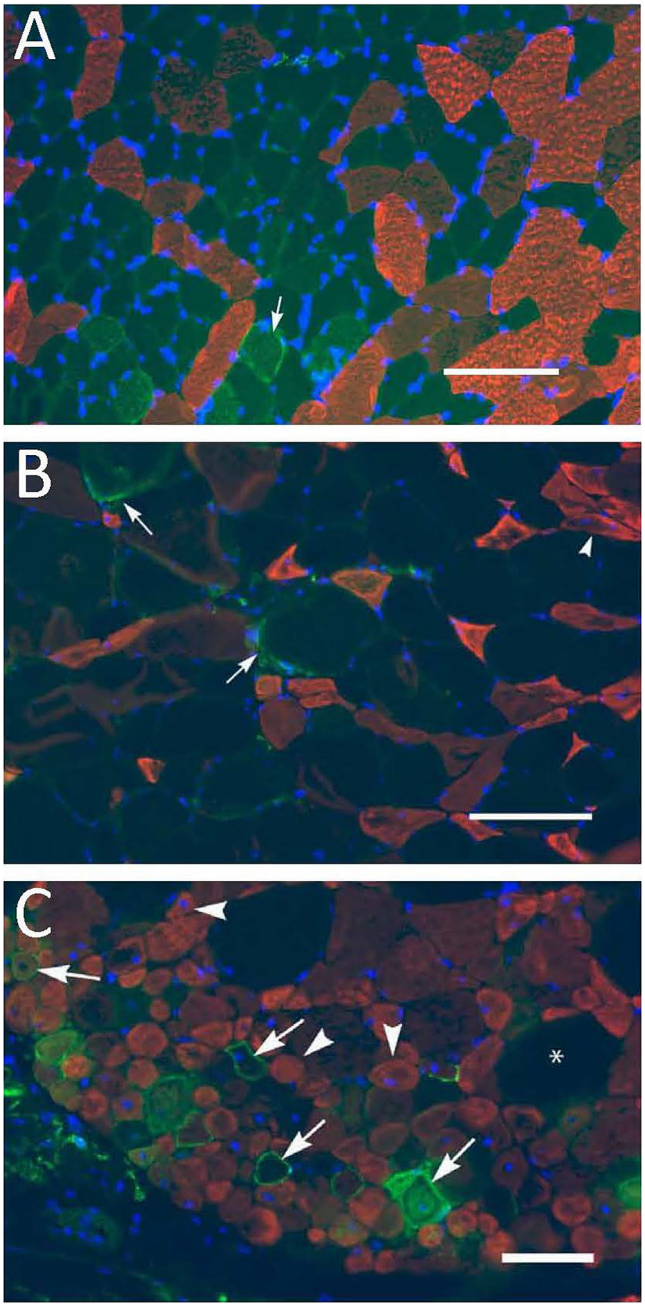

Fig. 7 – Representative triceps surae cross-sections showing: (A) the mid/deep-region of the gastrocnemius of an HR line 8 (non-mini) mouse; (B) the mid-region of the gastrocnemius of an HR line 3 mini-muscle mouse, and (C) the superficial region of the gastrocnemius of an HR line 3 mini-muscle mouse triple stained for MyHC-2b with antibody BF-F3 (red), the neural cell adhesion molecule (NCAM) (green), and nuclei (blue). (A) In the non-mini-muscle mouse, the mid/deep-region of the gastrocnemius contains several large MyHC-2b positive fibers (red fibers) and several fibers that are negative for MyHC-2b (unstained). Some fibers (arrow) have a light NCAM staining (green) on the periphery (scale bar in A = 100 μm). (B) In the mini-muscle mouse, the mid-region of the gastrocnemius contains several small 'angular' MyHC-2b positive fibers (red fibers), many with central nuclei (white arrowhead) and several fibers that are negative for MyHC-2b with peripheral nuclei (unstained). A few fibers (white arrows) show a light NCAM staining (green) on the fiber periphery (scale bar in B = 50 μm). (C) In the superficial region of the gastrocnemius of the mini-muscle mouse, many small 'rounded' MyHC-2b positive fibers, many of which have central nuclei, are present (white arrowheads). This region contains a few fibers that are negative for MyHC-2b with peripheral nuclei (unstained). Several, but not the majority of small 'rounded' MyHC-2b fibers, have a distinct NCAM staining on the periphery of the fiber (white arrows) (scale bar in C = 50 μm).

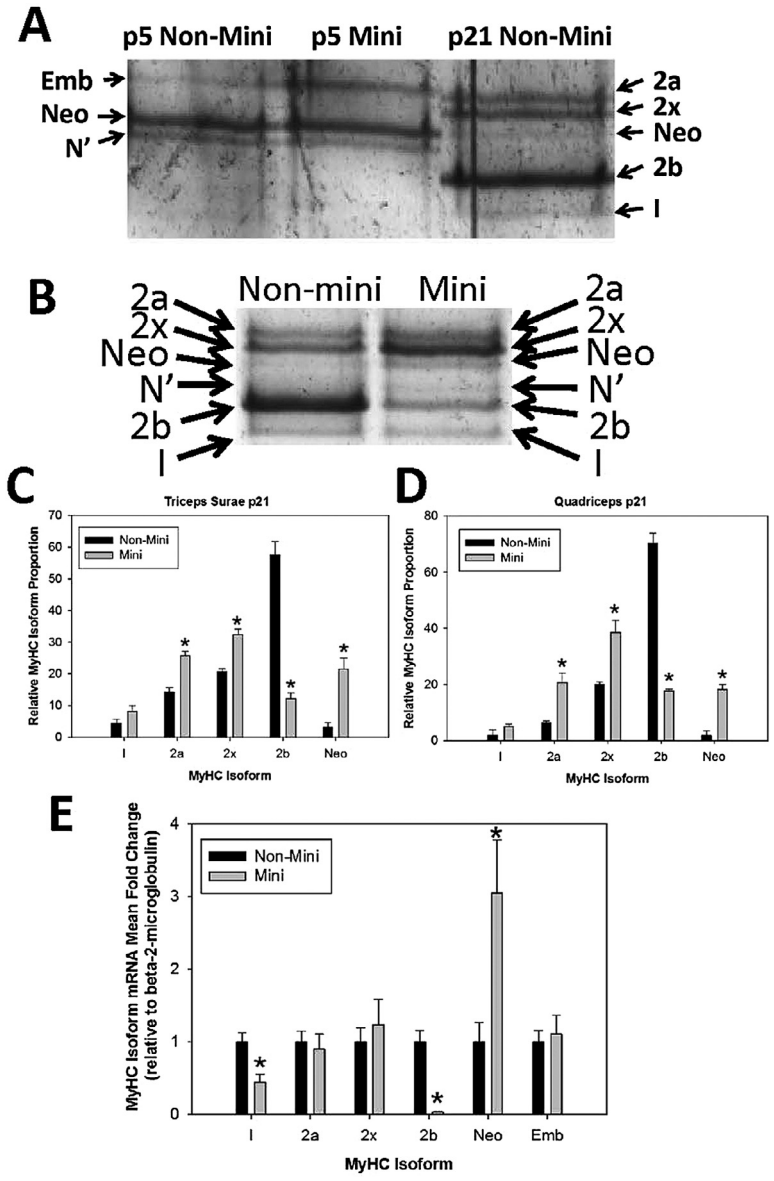

Fig. 8 – (A) A representative high resolution SDS-PAGE gel showing the MyHC-isoforms of neonatal p5 (5-day old) lower hindlimb muscle (all of the muscle from the calf region was excised together in order obtain sufficient amounts of muscle protein). Each lane contains a single representative sample from a high-running line 8 (Non-Mini) and a line 3 mini-muscle (Mini) mouse. The three MyHC isoforms present in the p5 samples were MyHC-embryonic (Emb), MyHC-neonatal (Neo) and a third band (N′) which appears to be present only in neonatal samples. The identities of the adult isoforms are shown at left and in a p21 (21-day old) triceps surae sample (p21 Non-Mini) for comparison. Notice the relative similarity in MyHC isoforms in p5 Non-Mini and p5 Mini suggesting that the changes in MyHC isoforms are not evident at p5. (B) Representative high resolution SDS-PAGE gel showing the MyHC-isoforms of juvenile p21 (21-day old) triceps surae muscle. Each lane contains a single representative sample from a high-running line 8 (Non-mini) and a line 3 mini-muscle (Mini) mouse. The MyHC isoforms present in the p21 samples were MyHCs-2a, -2x, -Neo, -N′, -2b and –I, as shown. Notice the reduced level MyHC-2b and increased level of MyHC-Neo in the mini-muscle mouse sample. (C and D) Quantification of MyHC isoforms in the p21 non-mini and mini-muscle mice (for simplicity the MyHC-Neo and MyHC-N′ bands were added together and expressed as MyHC-Neo). The bars represent the mean values +/– the SEM. The asterisk denotes significantly different from non-mini at $p \leq 0.05$. (E) MyHC isoform mRNA levels in the triceps surae muscle group of juvenile p21 non-mini-muscle (Non-Mini) and mini-muscle (Mini) mice. Real-time RT-PCR was used to quantify MyHC-I, -2a, -2x, -2b, -neonatal (Neo), and -embryonic (Emb) mRNA levels. The bars represent the mean values +/– the SEM. The asterisk denotes significantly different from both non-mini groups at $p \leq 0.05$.

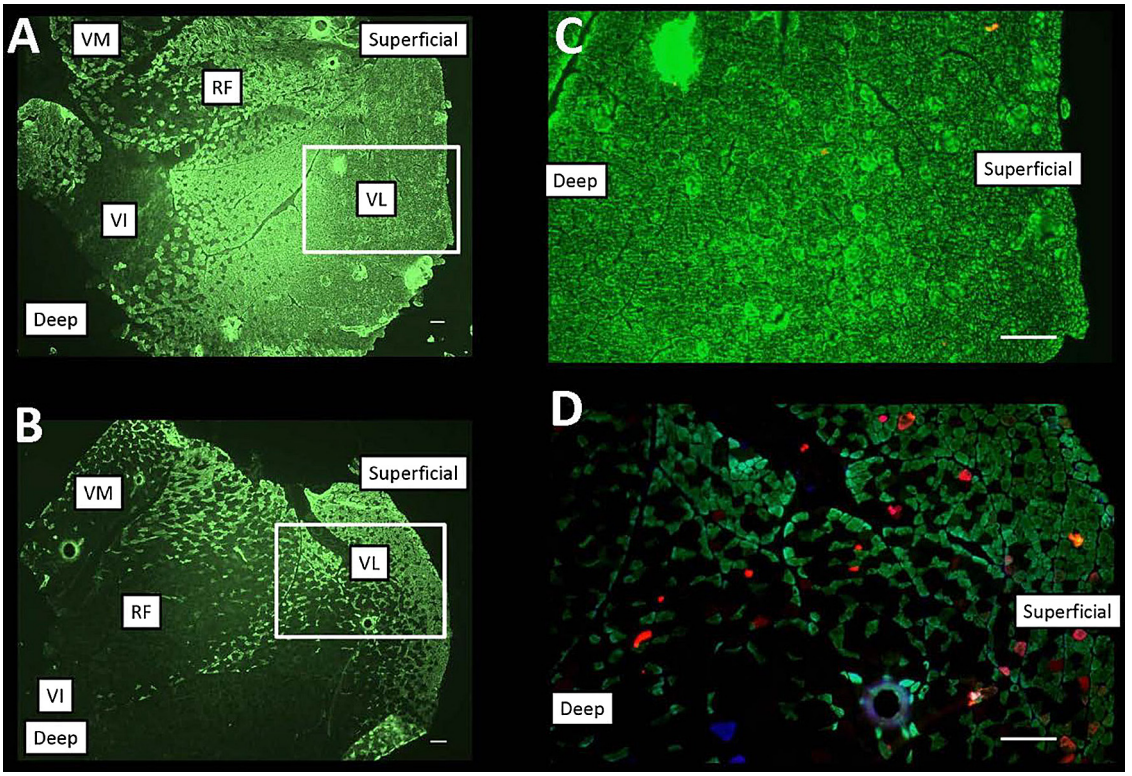

Fig. 9 – Representative whole quadriceps cross-sections immunochemically stained for MyHC-2b (green). (A) HR line 8 (non-mini-muscle) mouse; (B) line 3 mini-muscle mouse. The specific quadriceps muscles, vastus medialis (VM), vastus lateralis (VL), vastus intermedius (VI), and rectus femoris (RF) are identified, as well as the superficial and deep regions. Note the high level of green staining (presence of MyHC-2b) throughout the non-mini-muscle (A), but not the mini-muscle (B) quadriceps. The superficial region of the non-mini-muscle mouse (A) is virtually entirely composed of MyHC-2b fibers, which are less plentiful in the mini-muscle mouse (B). High-magnification of the vastus lateralis (see the boxed regions of A and B) immunochemically stained for MyHC-2b (green), MyHC-2a (blue) and MyHC-I (red) are shown in (C) HR line 8 (non-mini-muscle) mouse and (D) line 3 mini-muscle mouse. Again, note the high level of green staining (presence of MyHC-2b) throughout the non-mini-muscle (C), but not the mini-muscle (D) VL. The entire superficial region of the non-mini-muscle mouse (C) is composed of MyHC-2b fibers that extend to the deeper region (left). In contrast a high proportion of fibers remain unstained (likely containing MyHC-2x) in the mini-muscle mouse VL, although a few MyHC-I and -2a fibers are also present (D). The scale bars represent 100 μm for all sections.

elevated activity of the bidirectional promoter between the MyHC-2b and neonatal genes, suppressing MyHC-2b and elevating MyHC-neonatal at a crucial time point in maturation (perhaps before p21), hence resulting in a maintenance of MyHC-neonatal expression and immature 2b fibers. In fact, it was previously demonstrated that the MyHC-2b NAR (termed the "bII NAT" by Pandorf et al., 2012) was decreased whereas the MyHC-2b pre-mRNA and mature mRNA were increased from 10–20 days of age in rats; moreover, the levels of the MyHC-2b NAR were positively correlated with the levels of the MyHC-neonatal pre-mRNA (Pandorf et al., 2012).

Finally, it is known that a family of micro-RNAs (miRs) are involved in the fine regulation of MyHC isoform expression in both cardiac and skeletal muscle (McCarthy et al., 2009; Roth, 2011; van Rooij et al., 2009). It is possible that disruption of one of the miRs or a binding site for a miR could alter the expression of MyHC-2b directly and/or indirectly by influencing the expression of fiber-type specific transcriptional proteins.

In summary, both locomotor and non-locomotor muscles of mini-muscle mice show a reduction in MyHC-2b content. Although an apparently normal MyHC-2b protein is expressed in the mini-muscle mice, its reduced expression is limited to, and perhaps contributes to smaller fibers in locomotor muscles. Interestingly, the MyHC-2b positive fibers in the masseter muscle located in the jaw did not show a reduction in size, although they appeared to stain more lightly for MyHC-2b. Future studies will address the developmental differences between jaw and limb muscles in the mini-muscle mice.

Further analyses of the molecular and cellular mechanisms that cause the reduction in MyHC-2b should help facilitate the identification of the molecular mechanisms associated with the mini-muscle phenotype, as well as general mechanisms associated with the genetic (and heritable) regulation of adult fiber phenotype and fiber size (i.e., fiber maturation). Therefore, future studies will assess the role of the SNP in the cellular and molecular mechanisms

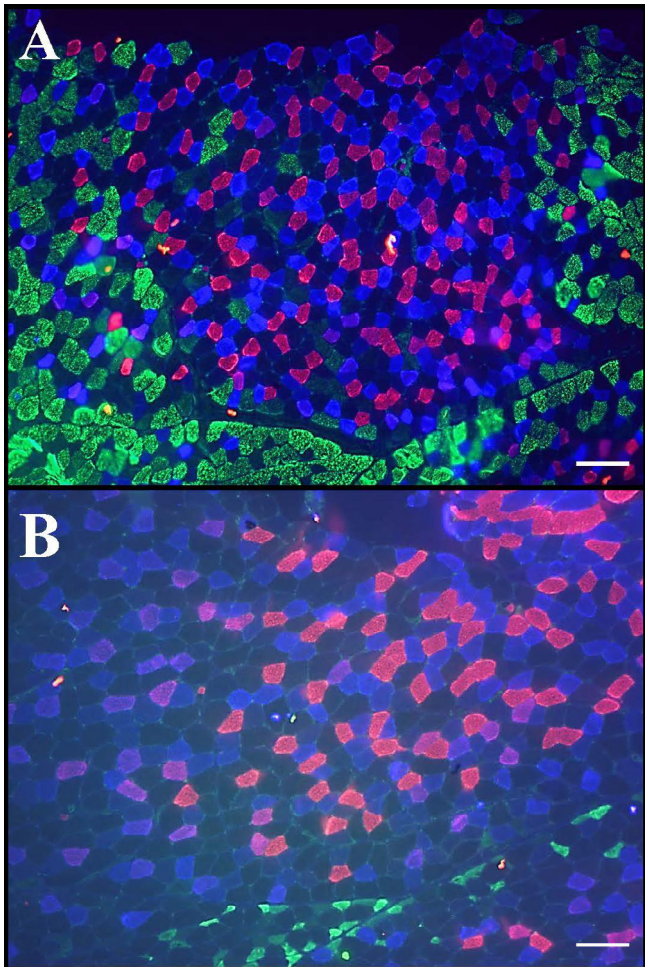

Fig. 10 – High magnification view of the vastus intermedius (VI) immunochemically stained for MyHC-2b (green), MyHC-2a (blue) and MyHC-I (red). (A) HR line 8 (non-mini-muscle) mouse; (B) line 3 mini-muscle mouse. Even in this deeply located muscle of the quadriceps, note the greater level of green staining (presence of MyHC-2b) throughout much of the non-mini-muscle (A), but not the mini-muscle (B) VI. The mini-muscle VI (B) contains primarily MyHC-I (red), -2a (blue), and-2d/x (unstained, black) fibers. Interestingly, in the non-mini-muscle mouse (A), the MyHC-2b fibers are characteristically larger than the other fiber types; whereas, in the mini-muscle mouse (B), the few MyHC-2b fibers present (towards the muscle periphery, at bottom) appear smaller than the other fiber types. The scale bars represent 100 μm for both sections.

associated with a reduction in MyHC-2b expression in the jaw and limb muscles of mini-muscle mice.

Author contributions

RJT and TG Jr., designed the research, performed statistical analyses, prepared the figures, and wrote the manuscript. RJT performed SDS-PAGE, mRNA and immunohistochemical analyses. WA maintained the mouse colony and performed muscle dissections. All authors read, edited, and approved the final manuscript.

Acknowledgements

This study was supported by a United States National Science Foundation grant (IOS-1121273) to Dr. Theodore Garland, Jr. Monoclonal antibodies SC-71 and BF-F3 developed by Dr. S. Schiaffino and F30 developed by Dr. F.E. Stockdale were obtained from the Developmental Studies Hybridoma Bank developed under the auspices of the NICHD and maintained by the University of Iowa, Department of Biology, Iowa City, IA 52242. Additional members of the Garland lab helped maintain the breeding colony and produce mice used in these studies.

REFERENCES

Acakpo-Satchivi, L.J., Edelmann, W., Sartorius, C., Lu, B.D., Wahr, P.A., Watkins, S.C., et al., 1997. Growth and muscle defects in mice lacking adult myosin heavy chain genes. J. Cell Biol. 139, 1219–1229.

Adams, G.R., McCue, S.A., Zeng, M., Baldwin, K.M., 1999. Timecourse of myosin heavy chain transitions in neonatal rats: importance of innervation and thyroid state. Am. J. Physiol. Regul. Integr. Comp. Physiol. 276, R954–R961.

Adams, G.R., Haddad, F., McCue, S.A., Bodell, P.W., Zeng, M., Qin, L., et al., 2000. Effects of spaceflight and thyroid deficiency on rat hindlimb development. II. Expression of MHC isoforms. J. Appl. Physiol. 88, 904–916.

Agbulut, O., Noirez, P., Beaumont, F., Butler-Browne, G., 2003. Myosin heavy chain isoforms in postnatal muscle development of mice. Biol. Cell 95, 399–406.

Allen, D.L., Harrison, B.C., Leinwand, L.A., 2000. Inactivation of myosin heavy chain genes in the mouse: diverse and unexpected phenotypes. Microsc. Res. Tech. 50, 492–499.

Allen, D.L., Harrison, B.C., Sartorius, C., Byrnes, W.C., Leinwand, L.A., 2001. Mutation of the IIB myosin heavy chain gene results in muscle fiber loss and compensatory hypertrophy. Am. J. Physiol. Cell Physiol. 280, C637–C645.

Bilodeau, G.M., Guderley, H., Joanisse, D.R., Garland, T., 2009. Reduction of type IIb myosin and IIB fibers in tibialis anterior muscle of mini-muscle mice from high-activity lines. J. Exp. Zool. A Ecol. Genet. Physiol. 311, 189–198.

Burniston, J.G., Meek, T.H., Pandey, S.N., Broitman-Maduro, G., Maduro, M.F., Bronikowski, A.M., et al., 2013. Gene expression profiling of gastrocnemius of "minimuscle" mice. Physiol. Genomics 45, 228–236.

Canepari, M., Pellegrino, M.A., D'Antona, G., Bottinelli, R., 2010. Skeletal muscle fibre diversity and the underlying mechanisms. Acta Physiol. (Oxf.) 199, 465–476.

Careau, V., Wolak, M.E., Carter, P.A., Garland, T., Jr., 2013. Limits to behavioral evolution: the quantitative genetics of a complex trait under directional selection. Evolution 67, 3102–3119.

Condon, K., Silberstein, L., Blau, H.M., Thompson, W.J., 1990. Development of muscle fiber types in the prenatal rat hindlimb. Dev. Biol. 138, 256–274.

di Maso, N.A., Caiozzo, V.J., Baldwin, K.M., 1999. Single-fiber myosin heavy chain polymorphism during postnatal development: modulation by hypothyroidism. Am. J. Physiol. Regul. Integr. Comp. Physiol. 278, R1099–R1106.

Dlugosz, E.M., Chappell, M.A., McGillivray, D.G., Syme, D.A., Garland, T., 2009. Locomotor trade-offs in mice selectively bred for high voluntary wheel running. J. Exp. Biol. 212, 2612–2618.

Garland, T., Morgan, M.T., Swallow, J.G., Rhodes, J.S., Girard, I., Belter, J.G., et al., 2002. Evolution of a small-muscle polymorphism in lines of house mice selected for high activity levels. Evolution 56, 1267–1275.

Garland, T., Kelly, S.A., Malisch, J.L., Kolb, E.M., Hannon, R.M., Keeney, B.K., et al., 2011. How to run far: multiple solutions and sex-specific responses to selective breeding for high voluntary activity levels. Proc. Biol. Sci. 278, 574–581.

Gordon, T., Ly, V., Hegedus, J., Tyreman, N., 2009. Early detection of denervated muscle fibers in hindlimb muscles after sciatic nerve transection in wild type mice and in the G93A mouse model of amyotrophic lateral sclerosis. Neurol. Res. 31, 28–42.

Guderley, H., Houle-Leroy, P., Diffee, G.M., Camp, D.M., Garland, T., 2006. Morphometry, ultrastructure, myosin isoforms, and metabolic capacities of the "mini muscles" favoured by selection for high activity in house mice. Comp. Biochem. Physiol. B Biochem Mol. Biol. 144, 271–282.

Haddad, F., Qin, A.X., Giger, J.M., Guo, H., Baldwin, K.M., 2007. Potential pitfalls in the accuracy of analysis of natural sense-antisense RNA pairs by reverse transcription-PCR. BMC Biotechnol. 7, 21.

Hannon, R.M., Kelly, S.A., Middleton, K.M., Kolb, E.M., Pomp, D., Garland, T., Jr., 2008. Phenotypic effects of the "mini-muscle" allele in a large HR x C57Bl/6J mouse backcross. J. Hered. 99, 349–354.

Hartmann, J., Garland, T., Hannon, R.M., Kelly, S.A., Munoz, G., Pomp, D., 2008. Fine mapping of "mini-muscle," a recessive mutation causing reduced hindlimb muscle mass in mice. J. Hered. 99, 679–687.

Houle-Leroy, P., Guderley, H., Swallow, J.G., Garland, T., 2003. Artificial selection for high activity favors mighty mini-muscles in house mice. Am. J. Physiol. Regul. Integr. Comp. Physiol. 284, R433–R443.

Kelly, S.A., Bell, T.A., Selitsky, S.R., Buus, R.J., Hua, K., Weinstock, G.M., et al., 2013. A novel intronic single nucleotide polymorphism in the myosin heavy polypetide 4 gene is responsible for the mini-muscle phenotype characterized by a major reduction in hind-limb muscle mass in mice. Genetics 195, 1385–1395.

Laemmli, U.K., 1970. Cleavage of structural proteins during the assembly of the head of bacteriophage T4. Nature 227, 680–685.

Livak, K.J., Schmittgen, T.D., 2001. Analysis of relative gene expression data using real-time quantitative PCR and the $2^{-\Delta\Delta CT}$ Method. Methods 25, 402–408.

Malisch, J.L., Breuner, C.W., Kolb, E.M., Wada, H., Hannon, R.M., Chappell, M.A., et al., 2009. Behavioral despair and home-cage activity in mice with chronically elevated baseline corticosterone concentrations. Behav. Genet. 39, 192–201.

McCarthy, J.J., Esser, K.A., Peterson, C.A., Dupont-Versteegden, E.E., 2009. Evidence of MyomiR network regulation of beta-myosin heavy chain gene expression during skeletal muscle atrophy. Physiol. Genomics 39, 219–226.

McGillivray, D.G., Garland, T., Dlugosz, E.M., Chappell, M.A., Syme, D.A., 2009a. Changes in efficiency and myosin expression in the small-muscle phenotype of mice selectively bred for high voluntary running activity. J. Exp. Biol. 212, 977–985.

McGillivray, D.G., Garland, T., Dlugosz, E.M., Chappell, M.A., Syme, D.A., 2009b. Changes in efficiency and myosin expression in the small-muscle phenotype of mice selectively bred for high voluntary running activity. J. Exp. Biol. 212, 977–985.

Middleton, K.M., Kelly, S.A., Garland, T., 2008. Selective breeding as a tool to probe skeletal response to high voluntary locomotor activity in mice. Integr. Comp. Biol. 48, 394–410.

Mizunoya, W., Wakamatsu, J., Tatsumi, R., Ikeuchi, Y., 2008. Protocol for high-resolution separation of rodent myosin heavy chain isoforms in a mini-gel electrophoresis system. Anal. Biochem. 377, 111–113.

Pandorf, C.E., Haddad, F., Roy, R.R., Qin, A.X., Edgerton, V.R., Baldwin, K.M., 2006. Dynamics of myosin heavy chain gene regulation in slow skeletal muscle: role of natural antisense RNA. J. Biol. Chem. 281, 38330–38342.

Pandorf, C.E., Jiang, W., Qin, A.X., Bodell, P.W., Baldwin, K.M., Haddad, F., 2012. Regulation of an antisense RNA with the transition of neonatal to IIb myosin heavy chain during postnatal development and hypothyroidism in rat skeletal muscle. Am. J. Physiol. Regul. Integr. Comp. Physiol. 302, R854–R867.

Pette, D., Vrbova, G., 1992. Adaptation of mammalian skeletal muscle fibers to chronic electrical stimulation. Rev. Physiol. Biochem. Pharmacol. 120, 115–202.

Ribaric, S., Cebasek, V., 2013. Simultaneous visualization of myosin heavy chain isoforms in single muscle sections. Cells Tissues Organs 197, 312–321.

Rinaldi, C., Haddad, F., Bodell, P.W., Qin, A.X., Jiang, W., Baldwin, K.M., 2008. Intergenic bidirectional promoter and cooperative regulation of the IIx and IIb genes in fast skeletal muscle. Am. J. Physiol. Regul. Integr. Comp. Physiol. 295, R208–R218.

Rivero, J.L., Talmadge, R.J., Edgerton, V.R., 1998. Fibre size and metabolic properties of myosin heavy chain-based fibre types in rat skeletal muscle. J. Muscle Res. Cell Motil. 19, 733–742.

Rivero, J.L., Talmadge, R.J., Edgerton, V.R., 1999. Interrelationships of myofibrillar ATPase activity and metabolic properties of myosin heavy chain-based fibre types in rat skeletal muscle. Histochem. Cell Biol. 111, 277–287.

Roth, S.M., 2011. MicroRNAs: playing a big role in explaining skeletal muscle adaptation? J. Appl. Physiol. 110, 301–302.

Roy, R.R., Baldwin, K.M., Edgerton, V.R., 1991. The plasticity of skeletal muscle: effects of neuromuscular activity. Exerc. Sport Sci. Rev. 19, 269–312.

Sartorius, C.A., Lu, B.D., Acakpo-Satchivi, L., Jacobsen, R.P., Byrnes, W.C., Leinwand, L.A., 1998. Myosin heavy chains IIa and IId are functionally distinct in the mouse. J. Cell Biol. 141, 943–953.

Schiaffino, S., Reggiani, C., 2011. Fiber types in mammalian skeletal muscles. Physiol. Rev. 91, 1447–1531.

Swallow, J.G., Carter, P.A., Garland, T., 1998. Artificial selection for increased wheel-running behavior in house mice. Behav. Genet. 28, 227–237.

Syme, D.A., Evashuk, K., Grintuch, B., Rezende, E.L., Garland, T., 2005. Contractile abilities of normal and "mini" triceps surae muscles from mice (Mus domesticus) selectively bred for high voluntary wheel running. J. Appl. Physiol. 99, 1308–1316.

Talmadge, R.J., 2000. Myosin heavy chain isoform expression following reduced neuromuscular activity: potential regulatory mechanisms. Muscle Nerve 23, 661–679.

Talmadge, R.J., Roy, R.R., 1993. Electrophoretic separation of rat skeletal muscle myosin heavy-chain isoforms. J. Appl. Physiol. 75, 2337–2340.

Talmadge, R.J., Roy, R.R., Edgerton, V.R., 1995. Prominence of myosin heavy chain hybrid fibers in soleus muscle of spinal cord-transected rats. J. Appl. Physiol. 78, 1256–1265.

Thomason, D.B., Baldwin, K.M., Herrick, R.E., 1986. Myosin isozyme distribution in rodent hindlimb skeletal muscle. J. Appl. Physiol. 60, 1923–1931.

van Rooij, R.E., Quiat, D., Johnson, B.A., Sutherland, L.B., Qi, X., Richardson, J.A., et al., 2009. A family of microRNAs encoded by myosin genes governs myosin expression and muscle performance. Dev. Cell 17, 662–673.

Whalen, R.G., Harris, J.B., Butler-Browne, G.S., Sesodia, S., 1990. Expression of myosin isoforms during notexin-induced regeneration of rat soleus muscles. Dev. Biol. 141, 24–40.

Yoon, S.J., Seiler, S.H., Kucherlapati, R., Leinwand, L., 1992. Organization of the human skeletal myosin heavy chain gene cluster. Proc. Natl Acad. Sci. U.S.A. 89, 12078–12082.